Mon. Not. R. Astron. Soc. **000**, 000–000 (2003)

The Local Hole in the Galaxy Distribution: New Optical Evidence

G.S. Busswell, T. Shanks, P.J. Outram, W.J. Frith, N. Metcalfe & R. Fong
Department of Physics, University of Durham, Science Labs, South Road, Durham DH1 3LE, United Kingdom

19 February 2003

ABSTRACT

We present a new CCD survey of bright galaxies predominantly within the Northern and Southern strips of the 2dF Galaxy Redshift Survey (2dFGRS) areas. We use the new CCD data to check the photographic photometry scales of the 2dFGRS, APM Bright Galaxy Catalogue, APM-Stromlo Redshift Survey, Durham-UKST (DUKST) survey, Millenium Galaxy Catalogue (MGC) and Sloan Digital Sky Survey (SDSS). We find evidence for scale and zero-point errors in the 2dFGRS northern field, DUKST and APM data of 0.10, 0.24 and 0.31 mag. respectively; we find excellent agreement with the MGC and SDSS photometry. We use our CTIO data to correct the photographic photometry, we then compare the CCD number counts in both the Northern and Southern survey areas. We find conclusive evidence that the Southern counts with B<17 mag are down by ≈30 per cent relative to both the Northern counts and to the models of Metcalfe et al in the same magnitude range. We further compare the number redshift distributions from the B< 17 mag Durham-UKST and B<19.5 2dFGRS redshift surveys using the corrected photometry. While the Northern n(z) from 2dFGRS appears relatively homogeneous over its whole range, the Southern n(z) shows a 30 per cent deficiency out to z=0.1; at higher redshifts it agrees much better with the Northern n(z) and the homogeneous model n(z). The Durham-UKST n(z) shows that the Southern 'hole' extends over a 20×75 deg^2 area. The troughs with z<0.1 in the Durham-UKST n(z) appear deeper than for the fainter 2dFGRS data. This effect appears to be real since the troughs also appear to deepen in the 2dFGRS data when magnitude limited at B<17 mag and so this may be evidence that the local galaxy distribution is biased on $\gtrsim 50\,h^{-1}$ Mpc scales which is unexpected in a ΛCDM cosmology. Finally, since the Southern local void persists over the full area of the APM and APM Bright Galaxy Catalogue with a ≈25 per cent deficiency in the counts below B≈17, this means that its extent is approximately 300 h^{-1}Mpc×300 h^{-1}Mpc on the sky as well as ≈300 h^{-1}Mpc in the redshift direction. Such a 25 per cent deficiency extending over ≈10^7 h^{-3} Mpc^3 may imply that the galaxy correlation function's power-law behaviour extends to ≈150 h^{-1}Mpc with no break and show more excess large-scale power than detected in the 2dFGRS correlation function or expected in the ΛCDM cosmology.

Key words: galaxies: surveys – galaxies: photometry – optical: galaxies – large-scale structure of the Universe

1 INTRODUCTION

It has been apparent for many years that the B galaxy number counts may be steeper at bright magnitudes than expected in a homogeneous, unevolving, cosmological model (Shanks et al. 1990). The counts appeared to have a Euclidean slope whereas the models predict a much flatter slope due to the expansion and the K-correction. Shanks et al. suggested that these steep counts maybe caused by large-scale galaxy clustering whereas other authors such as Maddox et al. (1990a) tended to favour the suggestion that the steepness was due to evolution. Both ideas had difficulties - the unevolved n(z) at B=17 and B=21 argued against galaxy luminosity evolution, while the local void would have to persist to almost $300h^{-1}$Mpc if the low number counts were caused by galaxy clustering.

Most of these authors used counts made from measurements of photographic plates. This meant that there remained the possibility that these observations were in error, due to non-linearities in the photographic magnitude scales. More recently it has become possible to survey large areas of the sky with linear CCD detectors. At first these were used

to calibrate the photographic magnitudes but this effort has been hindered by the quite large rms errors in the photographic photometry found even at relatively bright magnitudes. The CCD detectors are now large enough to provide the survey data by themselves and in this paper we describe a new survey primarily in the 2dF galaxy redshift survey areas, using the CTIO Curtis Schmidt CCD camera.

The advent of deeper galaxy redshift surveys such as 2dFGRS opens up a new possibility of investigating the scale at which the local hole ceases to dominate and the Universe appears to become homogeneous. In previous surveys such as the Durham-UKST Galaxy Redshift survey, the n(z) extended to z≈0.1 and it was found that count models which quite successfully fitted galaxy counts at B>18 did not fit the B<17 n(z) even in the range 0.05<z<0.1 which might have been thought to be safely outside any local inhomogeneities. The fact that the model n(z) over-predicted the observed n(z) all the way to z=0.1 meant that if the local void hypothesis was correct then the 'hole' in the galaxy distribution had to extend to z≈0.1 or r≈ $300\,h^{-1}$ Mpc.

In this paper we first present details of our observations and data reduction in Section 2. In section 3 we use our CTIO CCD data to check the calibration of several previous galaxy number counts so that the corrected results from the various authors can be compared to the CTIO counts themselves. In section 4 the CTIO counts are presented in each band. The number redshift distributions from the 2dF Galaxy Redshift Survey (2dFGRS; Colless et al. 2001) and the Durham-UKST Redshift Survey (Ratcliffe et al. 1998) are examined in Section 5 to investigate the possible existence of a 'local hole' in the galaxy distribution in the Southern Galactic Cap (SGC). A discussion follows in Section 6.

2 DATA REDUCTION

2.1 Observations

The observations were taken using the 0.6m Curtis Schmidt Telescope at CTIO, La Serena, Chile. We had two filters, Harris B and R, with magnitude limits of 20.5 and 19.5 respectively, and the imaging data was taken over 2 observing runs of 7 nights, each in excellent weather conditions. The North Galactic Cap (NGC) observations were taken from 8-14 April 1999 inclusive (observers GSB and TS), and the data in the South Galactic Cap (SGC) from 17-23 October 2000 inclusive (observers GSB and PJO). The CCD is a 2048x2048 24 micron chip with 2.3 arcsecond pixels, so that when the bias was subtracted this resulted in a 1.69 degree^2 field of view for each exposure.

In the NGC, we observed 3 main strips of sky in B and R at declinations of 0, -5 and -10 degrees, where the equatorial and -5 degree strips overlap with the 2dF Galaxy Redshift Survey (Colless et al. 2001). The strips were 1.3 degrees wide, which was dictated by the field of view of the telescope, and had an RA range from 9hrs. 45mins. up to 15hrs. The strips were joined at the ends by two smaller strips which were constant at declinations of 10hrs and 15 hrs. In total, this gave a potential 300 hundred square degrees of data in our B and R filters, assuming we had photometric conditions throughout all 7 nights.

In the SGC, we again observed in 3 main strips at constant declinations, this time at -28, -30 and -32, with the knowledge that this would completely overlap with the 2dFGRS fields. The ends of the strips were at RA's of 21hrs. 40mins. and 03hrs. 15mins. Because the strips were much closer together than in the NGC, it was possible to connect the strips by simply doing single exposures every half hour of RA at declinations of -29 and -31 degrees. In addition to these three long strips of $\sim$ 100 square degrees each, we also observed a shorter strip at a declination of -45 degrees from an RA of 02hrs. to 02hrs. 45mins. giving an area of $\sim$ 15 square degrees. In total this gave us an imaging area in the SGC of 337 square degrees.

The format of our observations would be to take two standard star frames of suitable Landolt equatorial fields in each band at the beginning, the middle and the end of each night. We would then begin the observations in our chosen field by taking an exposure in the R band for 120 seconds and stop the tracking of the telescope for 1 min 18 seconds (when observing in the North, 1 min. 30 secs. in the South), so that the sky moved over by one quarter of the CCD chip. This 1 min 18 seconds was sufficient to let the CCD read out which took $\sim$ 45 seconds. An exposure of the same length of time would then be taken in the B filter, and so on. The result would be a series of frames at a constant declination in the sky where each frame overlapped its adjacent frames in the same filter by about half a chip. We would typically be able to cover about 90 mins. of RA (30 deg^2) using this method before the sky was too far over and we would then move the telescope and begin again.

The bias was subtracted, images trimmed and bad pixels corrected using the IRAF quadproc package. Typically, five or six dawn and twilight flat field images were taken in each bandpass. A master flat field image was produced in each filter for each night by first using the imcombine routine to median together each of the dawn flats and evening flats separately. The resulting frames were then averaged to produce our B and R master flats for that night. By dividing the median-ed dawn and twilight flats we typically found a 1-2 per cent gradient from top to bottom of the resulting frame, implying an error of about 0.005-0.01 to our galaxy photometry due to this effect. The frames for a particular night in each filter were then flat-fielded using the IRAF ccdproc package and the appropriate flat-field master frame.

2.2 Photometric Analysis

The fact that adjacent frames of the same filter overlapped by half-a-chip meant that a detailed analysis of the photometric conditions throughout each night could be performed. The results of this photometric analysis are shown in Table 1. Given that the weather was so good during both observing runs we decided to enforce a relatively strict criterion to determine the nature of the observing conditions. A night was deemed partially photometric if two or more adjacent frames show significant offsets (> 0.1 mag) from each other when performing best fits to the magnitude residuals of the stars. If a particular night was deemed to be "partially photometric" then none of the frames were used on the strip where the > 0.1 magnitude offset was found.

In order to ensure accurate zero-point calibration our

NGC field		SGC field	
night	photometric?	night	photometric?
1	yes	1	yes
2	partial	2	yes
3	partial	3	yes
4	yes	4	partial
5	partial	5	yes
6	yes	6	yes
7	yes	7	no

Table 1. By using the fact that the frames in each filter overlap adjacent frames by half a chip, we were able to analyse the photometric conditions for each night. This table shows a summary of this analysis from the two observing runs in the North and South Galactic Caps respectively. In total our survey areas taken in photometric conditions were 255 and 297 square degrees for the NGC and SGC respectively.

strategy was to scale each frame based on its airmass relative to the first frame in the sequence. We found that, assuming photometric conditions, the cumulative magnitude offset across a whole sequence was consistent with the airmass variation from the first to the last frame. Since we enforced strict criteria on whether frames had been observed in photometric conditions, this assumption was justified. This also meant that the calibration of each frame was completely independent of all the others in the sequence, eliminating the possibility of the propagation of magnitude offset errors. To take these airmass variations into account the frames were scaled according to the equations:

$$f_B = 10^{0.209(X_{1_B} - X_{n_B})/2.5} \quad (1)$$

$$f_R = 10^{0.108(X_{1_R} - X_{n_R})/2.5} \quad (2)$$

where X_{1_B}, X_{n_B} are the air-masses in the first and nth frames in a B filter sequence and X_{1_R}, X_{n_R} the corresponding air-masses for the R filter. f_B and f_R are the scale factors for the B and R filters respectively and the values 0.209 and 0.108 are the quoted airmass coefficients in B and R for the CTIO observatory. By using high-mass standard star frames in the B and R filters we obtained values for the airmass coefficients of 0.19 and 0.10 respectively, in good agreement with the quoted values.

2.3 Standard Stars and the Colour Equation

Once the internal zero-points had been calibrated a global zero-point for each sequence had to be calculated. We did this by using the B and R magnitudes of the Landolt (1992) standards stars from our standard star frames which were taken at the beginning, middle and the end of each night using the fields SA101, SA107, and SA110. Our standard star exposure times were 10 secs. in R and 20 secs. in B. The IRAF fitparams routine was then used to determine the best fit zero-point offsets (b_1 and r_1) and colour-term coefficients (b_3 and r_3) for each band in the equations:

$$m_b = B + b_1 + b_2 * X_b + b_3 * (B - R) \quad (3)$$

$$m_r = R + r_1 + r_2 * X_r + r_3 * (B - R) \quad (4)$$

where B and R are the Landolt standard star magnitudes, X_b and X_r are the air-masses of the standard star frame for the B and R bands respectively and m_b, m_r are the calculated magnitudes of the stars. The parameters b_2 and r_2 are equal to 0.209 and 0.108 respectively and, as has been mentioned, are the quoted airmass coefficients for the CTIO observatory. We found typical values of 0.05 for b_3, the colour-term coefficient, but the error on this value was 0.04. Since this was comparable to b_3, which was itself small, we decided only to fit b_1 in the colour equation. Because of the same reasons we only fitted the R band zero-point offset, r_2 in equation 4. Since we did not use any colour terms in equations 3 and 4 all reduced magnitudes of our final sources will be in B and R_{kc}, as used by Landolt (1992). The mean of the b_1's and r_1's was calculated over all seven nights and our resulting colour equations were then:

$$m_b = B + 4.533(^{+}_{-}0.0053) + 0.209 * X_b \quad (5)$$

$$m_r = R + 4.203(^{+}_{-}0.0067) + 0.108 * X_r \quad (6)$$

We used the SEXtractor software package (Bertin et al. 1996) to measure the magnitudes of our sources and perform star/galaxy separation. The sources were extracted, sequence by sequence, and frame by frame in each sequence. The seeing stellar FWHM was first estimated for a particular frame with an initial call of SExtractor and then the objects were extracted with a second pass, making use of the calculated stellar FWHM. We used the MAG_BEST parameter in SExtractor for the source magnitudes and since we had at least two observations of each source because of our frame overlaps, the mean of the two magnitudes was used in order to minimize errors in the photometry. A cosmic ray was defined as being a source which appeared on one frame but on neither of the adjacent frames and these would not be included in our source catalogue, but written to a cosmic ray file.

2.4 Star/Galaxy Separation

Star/Galaxy classification was carried out using the SExtractor software. The parameter CLASS_STAR is assigned a particular value for a source which varies between 0 and 1 for galaxy and star-like sources respectively. For B<18 and R<17 the SExtraxtor CLASS_STAR parameter is a good separator of stars and galaxies with 91 per cent in B and 90 per cent in R of sources with either CLASS_STAR>0.9 or <0.1. The fact that we have two filters is useful since we get four attempts to classify a particular source (as we have overlaps in each filter) instead of two, and can consequently achieve lower errors on the CLASS_STAR parameter. A full account of this technique is given in Busswell (2001).

To verify our star/galaxy separation we have checked our results with other reliable external sources. We find a galaxy completeness of >90 per cent for B<18 when comparing our northern equatorial field with $\approx 90\mathrm{deg}^2$ of the currently available Sloan Digital Sky Survey (SDSS; Yasuda et al. 2001). Stellar contamination is consequently less than 10 per cent in this magnitude range; the star/galaxy separation begins to break down for B>18 as the stellar contamination increases. A similar trend is observed in the R-band data except the completeness begins to decrease at R=16.5, but is still equal to 84 per cent for R=17. A similar check

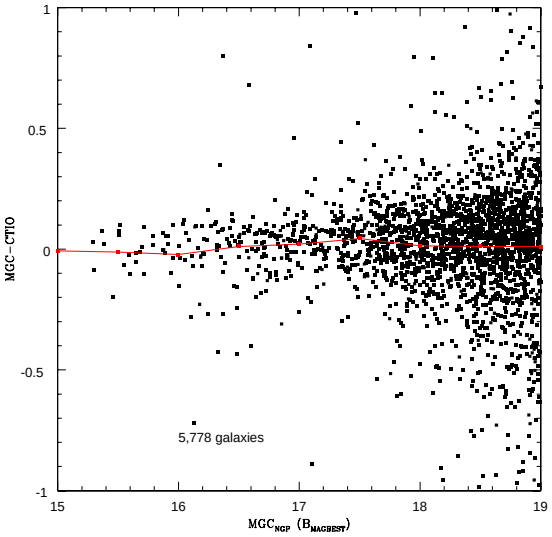

Figure 1. Our B-band CCD magnitudes are plotted against the residual of the MGC magnitudes and our magnitudes for galaxies common to both data-sets. The plot shows 5,778 galaxies and the black line connects the mean of the residual in each 0.5 magnitude bin. For B<18, we calculate a mean magnitude difference of MGC-CTIO=0.03 and a 1σ scatter of 0.1 about this value. For B>18, our photometry errors are observed to increase, which is unavoidable given the length of our exposures and size of our pixels.

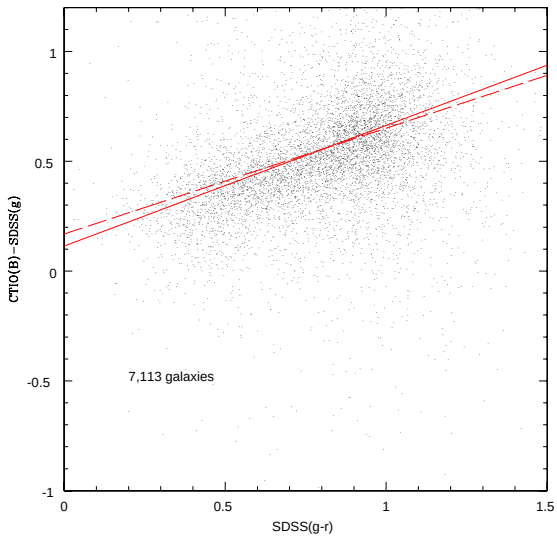

Figure 2. This plot shows the SDSS ($g^\star - r^\star$) vs. CTIO(B)-SDSS($g^\star$) for 7,133 galaxies in the 90 deg^2 overlap region. The solid line shows the best f it to the data and corresponds to a colour equation of $B = g^\star + 0.549(\pm0.07)(g^\star - r^\star) + 0.114$ as opposed to the relation $B = g^\star + 0.482(g^\star - r^\star) + 0.169$ (dashed line) quoted in Yasuda et al. (2001).

of the completeness with the Millennium Galaxy Catalogue (MGC; Driver - personal communication) in the B-band indicates a 100 per cent agreement in the source classification for B<16, with completeness and stellar contamination levels of 93 per cent and 5 per cent respectively at B=18. It should be noted that the MGC also used SEXtractor for the photometry and star/galaxy separation calculations.

3 CTIO CURTIS SCHMIDT CCD SURVEY

3.1 Photometry Comparisons

In order to check the accuracy of our photometry we have compared our galaxy sample with other very accurate data-sets. In Fig. 1 we show a comparison with the B-band MGC data for 5,778 matched galaxies over a 32 deg^2 area. The agreement is good, with negligible zero-point or scale errors. However, our magnitude errors can be seen to increase significantly for B>18.

We can make a similar comparison with the SDSS data (Yasuda et al. 2001) over the 90 square degree overlap region, using the g and r filters which need to be converted to our B Landolt band. The colour equation used in Yasuda et al. (2001) is:

$$B = g^\star + 0.482(g^\star - r^\star) + 0.169 \quad (7)$$

where $g^\star$ and $r^\star$ are in the AB magnitude system and the asterisks represent the fact that the SDSS photometry is preliminary. By plotting B-g* against $g^\star - r^\star$, shown in Fig 2 we can test this colour transformation for our galaxy sample. We in fact find the best fit line corresponds to the colour equation $B = g + 0.549(\pm0.07) * (g^\star - r^\star) + 0.114$. The discrepancy between the colour terms, which is consistent with the ±0.07 error, accounts for the 0.169-0.114=0.055 difference in the zero-point. In fact, if we insist on using the 0.482 colour term from Yasuda et al. (2001) then the zero-point difference (i.e. the average of the relation B-g*-0.482(g*-r*)-0.169 for all common galaxies between the SDSS and our CTIO survey) is less then 0.01 mag. The photometry system used for the SDSS data is new and the appropriate transformations to other band-passes are relatively poorly understood. This, combined with the fact that their photometry is still preliminary, could explain the discrepancy between the colour terms.

A comparison with the SDSS photometry, this time in the R Kron-Cousins pass-band, is shown in Fig. 3, where we have plotted the SDSS R_{kc} magnitude estimate against the magnitude difference SDSS(R_{kc})-CTIO(R_{kc}). The SDSS R_{kc} magnitude is calculated using the colour equation quoted in Blanton et al. (2001) of R_{GKC}=r* - 0.05 - 0.089(g*-r*). A further correction is performed using the relation R_{GKC}-R_{kc}=0.08 (Shectman et al. 1996) in order to obtain an estimate of the SDSS R_{kc} magnitude. We find excellent agreement over the magnitude range shown in Fig. 3, with a mean zero-point difference of SDSS(Rkc)-CTIO(R_{kc})=0.02($\pm$1 0.01).

Further checks of our R-band photometry in the NGC and comparisons to our B and R data in the SGC has been carried out in Busswell (2001) using data from Metcalfe et al. (1998) in the DARS GSA and GNB fields. This data shows an intrinsic scatter of 0.06 mags. in both B and R. Mean magnitude differences were found of -0.02$\pm$0.018, +0.02$\pm$0.02, and, -0.03$\pm$0.02 for comparisons to R-band data in the NGC and B-band and R-band data in the SGC respectively.

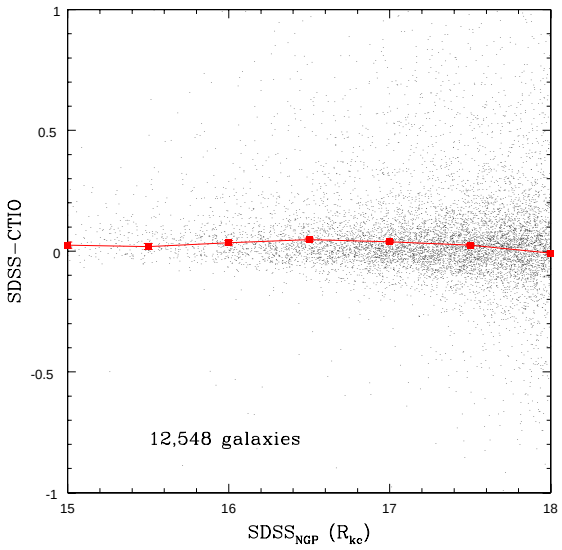

Figure 3. This plot shows a comparison with the SDSS photometry, but this time in our R Kron-Cousins pass-band. We have used the colour transformation, R_{GKC}=r*-0.05-0.089(g*-r*), quoted in Blanton et al. (2001) in order to transform to the R_{GKC} filter. The relation R_{GKC}-R_{kc}=0.08 is then used (Shectman et al. 1996) in order to obtain an SDSS magnitude estimate in our R Kron-Cousins filter. In this figure we have plotted the SDSS R_{kc} magnitude vs the quantity SDSS(R_{kc})-CTIO(R_{kc}) with the mean of the magnitude difference plotted in half magnitude bins. Excellent agreement is seen over the magnitude range shown with a mean zero-point difference of SDSS(R_{kc})-CTIO(R_{kc})=0.02($\pm$0.01)

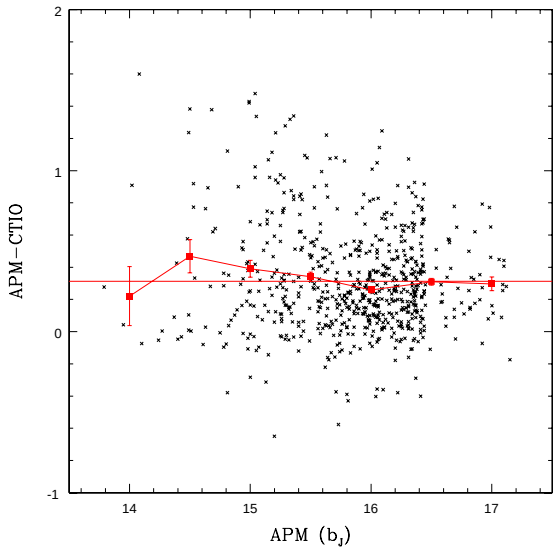

Figure 4. Comparison with the APMBGC and APMSRS galaxy photometry. Here we plot APM mag(b_J) vs APM(b_J)-CTIO(b_J) for all the APMBGC and APMSRS galaxies contained in our 297 deg^2 area. The points show the mean of the residual in 0.5 mag. bins and the solid line shows the mean zero-point offset over all our measured magnitudes which we calculate to be 0.313$\pm$0.01. The low sampling rate of the APMSRS is clearly illustrated, as the number of matched galaxies drops sharply as one moves to fainter magnitudes than b_J=16.44, the magnitude limit of the APMBGC.

3.2 The APM Bright Galaxy Photometry Correction

In order to investigate the APM photometry at bright magnitudes we have used our CTIO SGC data (our un-dust-corrected magnitudes), covering 297 deg^2, to check the accuracy of the publicly available APM Bright Galaxy Catalogue (APMBGC; Loveday et al. 1996)). This data reaches a magnitude limit of b_J=16.44 and so to reach slightly fainter magnitudes we have also used the publicly available photometry from the APM-Stromlo Redshift Survey (APMSRS), where the magnitude limit is b_J=17.15. We have converted our CTIO data to the b_J magnitude system using both our B Landolt and R Kron-Cousins data, in conjunction with the colour equation from Pimbblet et al. (2001):

$$b_J = B - 0.17(B - R) \quad (8)$$

Fig. 4 shows this comparison with the b_J mag. plotted vs the mag. difference APM-CTIO. In our 297 deg^2 survey area we find 629 matching galaxies with the APMBGC, which are of course brighter than b_J=16.44 and 96 matching galaxies with the APMSRS brighter than b_J=17.15. Note that the APMSRS has a sampling rate of 1/20 over the full 4300 deg^2 APM area and so we therefore expect to find 20 times more matched galaxies with the APMBGC than for the APMSRS in a given mag. interval. This low sampling rate is clearly illustrated in Fig. 4, where the number of matched galaxies drops sharply as one moves to fainter magnitudes than b_J=16.44, the magnitude limit of the APMBGC. We find a mean zero-point difference of APM-CTIO=0.313$\pm$0.01 mag. The difference is quite large and we will see in the discussion section what this 0.313 mag. correction could mean in terms of the implications for a hole in the SGC distribution of galaxies.

3.3 The Durham/UKST Photometry Correction

In this section we use our CTIO CCD photometry to check the accuracy of the Durham/UKST photometry. The DUKST redshift survey covers 1500 deg^2 in 4 strips and our CTIO SGC data overlaps with one of these 4 strips. The angular size of the survey is 20°x75° in the SGC to a limiting apparent magnitude of b_J=16.86. The catalogue consists of $\sim$2500 galaxy redshifts and therefore by comparing the model of Metcalfe et al. with the DUKST n(z) distribution, and taking into account any zero-point discrepancies with our CCD data, we can probe a larger area (1500 deg^2) in the SGC than the 2dFGRS can ($\sim$300 deg^2 at present). Although the DUKST will probe lower redshifts, the larger area will mean tighter constraints on the size and angular extent of the SGC deficiency in the galaxy distribution.

The DUKST galaxies were selected from the Edinburgh/Durham Southern Galaxy Catalogue (EDSGC: Collins, Heydon-Dumbleton & MacGillivray 1988). Ratcliffe et al. (1998) applied small corrections to the EDSGC b_J magnitudes in each of the 60 fields in an attempt to put them on the same zero-point scale of the APM catalogue. These corrections were calculated from results of Dalton et al. (1995) with the mean correction over all 60 fields,

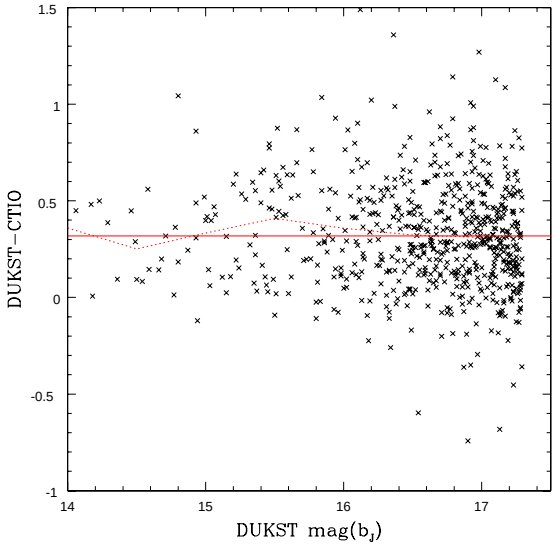

Figure 5. Here we plot EDGSC mag(b_J) vs EDGSC(b_J)-CTIO(b_J). The dotted line shows the mean of the residual in 0.5 mag. bins and the solid line shows the mean zero-point offset over all magnitudes which we calculate to be 0.310. In fact the mean offset between the EDSGC photometry and the APM data at b_J=19.5 is 0.07±0.11 for these 28 fields which overlap with our CTIO data as opposed to 0.05 for all 60 fields. This means that we find a 0.31-0.07=0.24±0.012 zero-point offset between our CCD photometry and the corrected EDSGC photometry used for the DUKST survey.

$< b_J^{APM} - b_J^{EDSGC} >$=- 0.05±0.11 mag. It should also be pointed out that the zero-point corrections were performed at b_J ∼19.5 as the APM is expected to give reliable photometry here. If this mean offset is to be believed in the magnitude range of the DUKST (b_J < 17), one is assuming there is no scale error in either the APM or EDSGC photometry.

Our CTIO SGC fields overlap with 28 of the 60 EDSGC fields and therefore we can make extensive tests of a large fraction of the DUKST photometry using our accurate CCD photometry. To convert to the DUKST b_J magnitude system we use our B Landolt and R Kron-Cousins photometry in conjunction with equation 8 (Pimbblet et al. 2001). In Fig. 5 we plot all the galaxies from each of the 28 fields in order to determine a mean zero-point offset. The dotted line shows the mean zero-point offset binned in half magnitude intervals and the solid line shows the mean zero-point offset over all magnitudes which we calculate to be 0.310. In fact the mean offset between the EDSGC photometry and the APM data at b_J=19.5 is 0.07 for the 28 fields which overlap with our CTIO data as opposed to 0.05 for all 60 fields. This means that we find a 0.31-0.07=0.24 zero-point offset between our CCD photometry and the corrected EDSGC photometry used for the DUKST survey. Although the DUKST photometry was corrected in order to be consistent with the zero-point of the APM, it is clear that there are discrepancies compared to our accurate CCD data. These zero-point differences appear field dependent although in some fields there are very few galaxies.

This mean zero-point offset between our CTIO CCD data and that of the DUKST may seem surprising given that the DUKST photometry has already been corrected/brightened by an average value of 0.05 mag. in order that it is consistent with the APM data at b_J=19.5 However, as we have already mentioned, any scale errors inherent in the APM or the DUKST could mean that this 0.05 correction may not apply at b_J <17. Our checks of the 2dFGRS photometry (based on the original APM data) showed up no significant scale error in the magnitude range 16 <b_J < 19.5 and therefore we claim that the problem lies with the EDSGC photometry used for the DUKST survey. A scale error of order 0.1 mag/mag in the range 17< b_J <19.5 would explain the 0.24 mag. discrepancy with our CCD data which we have found to be accurate to a few hundredths of a magnitude at B<17 from checks performed in Section 3.1.

3.4 Photometry Checks of the 2dFGRS

As described in Section 2, our 297 deg^2 SGC field is a complete subset of the southern 2dFGRS region. Therefore, providing our photometry is consistent with that of the 2dF, their SGC n(z) distribution can help us understand the exact nature of the apparent under-density observed relative to the galaxy count model of Metcalfe et al. (2001). Furthermore, for b_J >17, the 2dFGRS photometry has a zero-point that has changed slightly from the original APM data due to re-calibration with external CCD magnitudes. In the SGC this zero-point difference is very small, APM-2dFGRS=0.02 mag., and so any comparisons of our CTIO data with the 2dFGRS magnitudes will also be good checks of the original APM photometry for b_J > 17. In the NGC this zero-point difference is APM-2dFGRS=0.08 mag. (Cole priv. com.). In order to check how our photometry compares with that of the 2dFGRS we have matched all galaxies from the two surveys using matches within a 3.5″ radius. As in Section 4.1.1, we use both our B Landolt and R Kron-Cousins galaxy photometry in conjunction with the colour equation from Pimbblet et al. (2001) in order to convert to the 2dFGRS b_J filter. Figs. 6 and 7 show these comparisons for the NGC and SGC regions respectively. Note that in the NGC only ∼2/3 of our fields overlap with those of the 2dFGRS as opposed to 100 per cent in the SGC explaining the factor of ∼1.5 difference in the number of matching galaxies. We have plotted the 2dF b_J magnitude against the magnitude difference 2dF-CTIO for each field with the mean of the residual illustrated by the squares in each half magnitude bin. The 2dF galaxy photometry is of course based on that of the APM Galaxy Survey (Maddox et al. 1990a) with rms errors on the source magnitudes of 0.2-0.25 mag., and this can be seen via the large scatter around the mean in each magnitude bin. We have shown in Section 3.1 that our CCD photometry is much more accurate than this with rms errors of 0.1 mag. at B=18 and 0.05 mag. at B=16, and therefore we expect any zero-point and scale errors between the two surveys to be contained within the photographic 2dF data. The NGC comparison in Fig. 6 shows clear evidence of both a zero-point and scale error. We find good agreement at b_J=16 but the scale error induces a maximum zero-point error of 0.13 mag. at B=18 with a mean correction of 0.1 mag. for b_J >16. For the SGC field in Fig. 7 we find a much better agreement with no appreciable scale error and the mean of

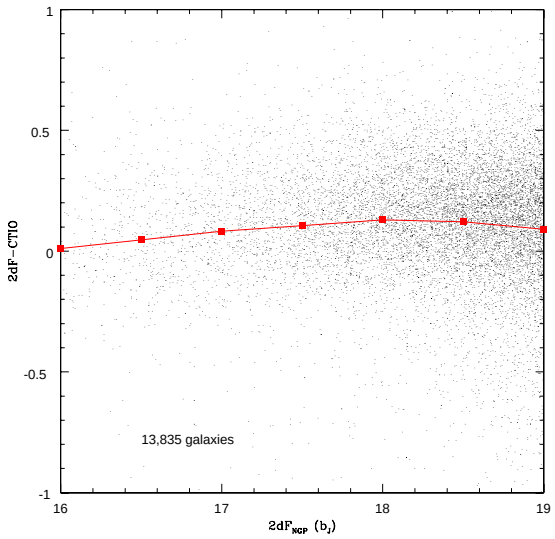

Figure 6. This plot shows 13,835 matching galaxies in the NGC from our CTIO survey and that of the 2dFGRS. We have plotted the 2dF b_J magnitude against the difference in magnitudes from the surveys, 2dF-CTIO, with the mean of this difference plotted in half magnitude bins. We converted the CTIO data to the 2dF b_J magnitude system using both our B Landolt and R Kron-Cousins band-passes in conjunction with the colour equation b_J=B-0.17(B-R) from Pimbblet et al. (2001). One can see a clear zero-point and scale error over the magnitude range shown with the zero-point difference peaking at 0.13 mag. when b_J=18. For $b_J > 16.0$ the mean correction is 0.1±0.005 mag.

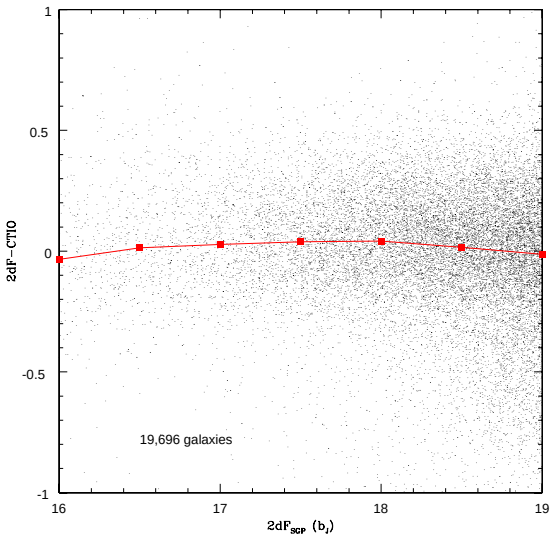

Figure 7. This plot shows 19,696 matching galaxies in the SGC from our CTIO survey and that of the 2dFGRS. We have plotted the 2dF b_J magnitude against the difference in magnitudes from the surveys, 2dF-CTIO, with the mean of this difference plotted in half magnitude bins. We converted the CTIO B-band data to the 2dF b_J magnitude system using both our B Landolt and R Kron-Cousins band-passes in conjunction with the colour equation b_J=B-0.17(B-R) from Pimbblet et al. (2001). The agreement in the SGC is good with the mean of the magnitude difference $< 0.05^{+}_{-}0.004$ mag. over the whole magnitude range shown.

the residuals agreeing to within 0.05 mag. over the whole magnitude range shown.

4 CTIO NUMBER COUNTS

Figs 8 and 9 show our CTIO galaxy number counts in the B and R bands respectively, which are both corrected for galactic extinction using the Schlegel et al. (1998) dust maps. Our B-band number counts in the NGC agree very well, firstly with the SDSS data in the magnitude range 16.5 <B< 18.5 and also with the MGC for 15.5 <B< 18.5. It should be noted that all three data sets were taken in overlapping regions of sky - a 32 and 90 deg^2 overlap with the MGC and SDSS data respectively in the NGC. Our CTIO data also overlaps with 163 deg^2 of the 2dFGRS in the NGC and 297 deg^2 in the SGC. Our SGC number counts agree extremely well with the 2dFGRS, which is important given the large overlap, but our NGC data is showing significantly more galaxies than that of the 2dF team. This could be due to real differences in the galaxy number density between the current 740 deg^2 2dF field and our 297 deg^2 field, or due to zero-point/scale differences in the galaxy photometry.

The shape and normalisation of our NGC number counts also agrees remarkably well with the no-evolution predictions of the low-q_0 model (see section 4.3 for model details) from B=18 to as bright as B=14. The shape of our B-band number counts in the SGC agrees well with our NGC data set, but the striking difference is that of the normalisation, which is calculated in each 0.5 magnitude interval in Table 2. We a find an average 30.7 per cent deficiency in galaxy numbers for our southern data compared to the north in the magnitude range 14<B<18. At B=19 this normalisation discrepancy has dropped to 17.3 per cent , although the galaxy incompleteness is a factor in this magnitude bin. The 2dF number counts also show a north-south difference, but only 20 per cent in galaxy numbers at B=18, with this difference virtually zero at B=19. The survey area of our SGC data was a subset of the 4300 deg^2 sky covered by the APM galaxy catalogue and our SGC number counts agree very well with the Metcalfe et al. (1995) corrected APM counts despite the order of magnitude less of sky coverage on our part. Our SGC number counts also agree well with the CCD data of Bertin & Dennefeld (1997), who cover 62 and 83 square degrees at high declinations ($|\delta| > 40^\circ$ in the North and South Galactic Caps respectively. Our CTIO counts, the 2dFGRS and MGC counts and those of Yasuda et al. have all been corrected for dust using the Schlegel et al. (1998) extinction maps. The APM and DUKST counts and those of Bertin & Dennefeld are not corrected for dust and the reason for this was that the vast majority of all these observations were in the SGP where it was orginally thought dust extinction was negligible. In fact Schlegel et al. predict values of 0.03 mag. in the B-band at the SGP and an average of 0.08 mag. over the whole SGC.

Our R-band galaxy counts show a similar trend in the normalisation difference, where the number discrepancies of the SGC counts relative to those in the SGC are tabulated in Table 3. The average percentage discrepancy is 22.2 per cent in the 13<R<17 range, and again this normalisation differ-

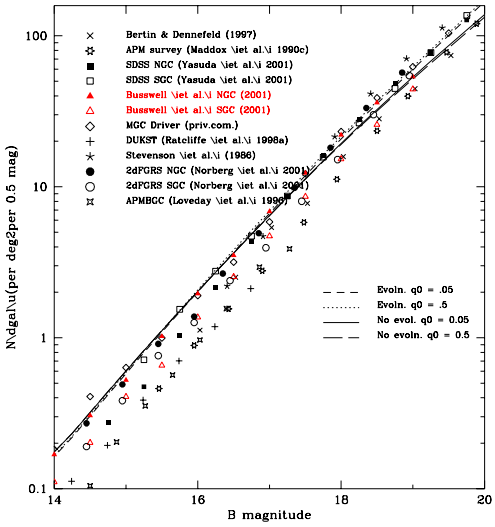

Figure 8. Our B band galaxy number counts. The filled and unfilled triangles show our number counts in the North and South Galactic Caps respectively. The filled and unfilled squares show the SDSS Commissioning Data in the Northern and Southern equatorial strips (Yasuda et al. 2001), the circles the 2dF Galaxy Redshift Survey (2dFGRS) data, the diamonds the Millenium Galaxy Catalogue (Driver priv. com.) results, the x's the data of Bertin & Dennefeld (1997) and the star-like symbols show the data of Stevenson et al. (1986). The APM counts (Maddox et al. 1990c) are indicated by the asterisk symbol and include the faint-end photometry correction of Metcalfe et al. (1995). The crosses show the Durham/UKST data of Ratcliffe et al. (1998) and the filled diamonds the APM bright galaxy data (for B<16.6 - for B>16.6 the APM-Stromlo counts are shown by the filled diamonds) of Loveday et al. (1996). The curves are Pure Luminosity Evolution (PLE) models of Metcalfe et al. (2001) and they are explained further in section 4.3. See text for details of dust corrections.

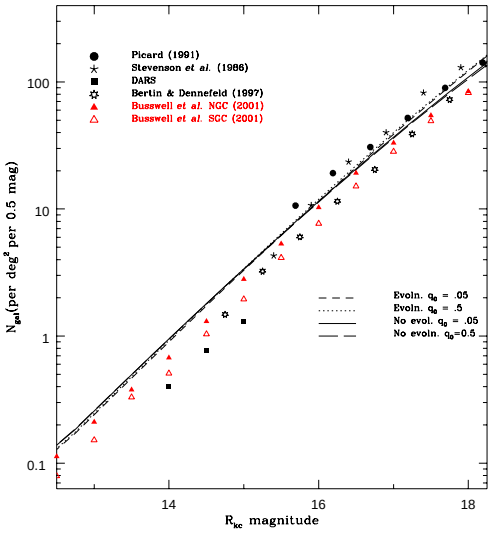

Figure 9. Our R band galaxy number counts. The filled and unfilled triangles show our number counts in the North and South Galactic Caps respectively. The filled circles show the data of Picard (1991), the skeleton stars that of Stevenson et al.(1986), the filled squares are the DARS data (Metcalfe et al. 1998) and the open stars show the data of Bertin & Dennefeld (1997). The curves are Pure Luminosity Evolution (PLE) models of Metcalfe et al. (2001) which assume the presence of dust in late type spiral galaxies. The models are explained further in section 4.3. See text for details of dust extinction corrections.

ence drops for fainter magnitudes. At R=18 there is only a 2.5 per cent discrepancy in the galaxy numbers, although galaxy incompleteness is again a factor. The shape of both the data sets in the 13<R<17 range is consistent with the no-evolution models, but there is a slight normalisation discrepancy in that all the data sets show less galaxies compared to the models for R< 15.5. There is a noticeable dip in both our number counts compared to the models between about R=13.5 and R=15.5 and there is good agreement with Bertin & Dennefeld, as in the B filter. Our data lies substantially below that of Picard et al. (1991), who cover 386 square degrees in both the NGC and SGC. In Fig. 8 our CTIO number counts have been corrected for dust using the Schlegel et al. (1998) extinction maps but none of the other data sets were de-reddened when originally published. This is because, either it was originally thought that a particular data-set suffered from negligible extinction, as in the case of the Stevenson points in the SGC, or the reddening correction was not known due to the absence of any accurate dust maps at the time of publication eg. Picard (1991).

Fig. 10 shows selected number count data with the appropriate zero-point corrections of 0.10 mag. to the 2dFGRS NGC data (for b_J >16.0), 0.24 mag. to that of the DUKST

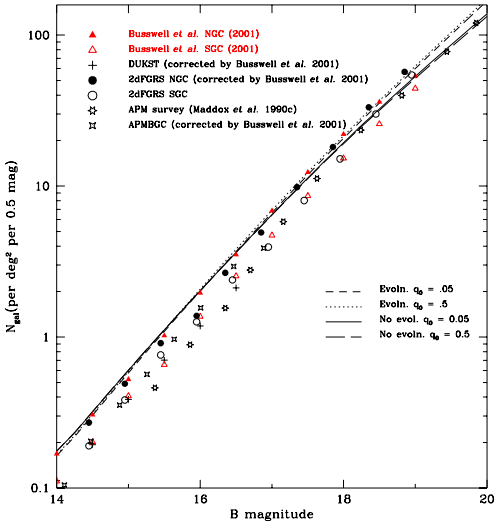

Figure 10. Here we show a similar plot to Fig. 8, but we impose the 0.313, 0.24, and 0.1 mag. photometry corrections derived for the APMBGC, DUKST and 2dF NGC data (for b_J >16.0) respectively. There is also a small 0.08 mag dust correction applied to the APM and APMBGC data (see text for details).

B	N_{gal}^{NGC}	N_{gal}^{SGC}	N-S discrepancy
12.25-12.75	0.031	0.017	45.2
12.75-13.25	0.047	0.024	48.9
13.25-13.75	0.066	0.067	-1.5
13.75-14.25	0.168	0.111	33.9
14.25-14.75	0.305	0.201	34.1
14.75-15.25	0.524	0.406	22.5
15.25-15.75	1.021	0.655	35.8
15.75-16.25	1.959	1.367	30.2
16.25-16.75	3.508	2.535	27.7
16.75-17.25	6.855	4.714	31.2
17.25-17.75	12.353	8.619	30.2
17.75-18.25	22.059	15.283	30.7
18.25-18.75	36.047	25.779	28.5
18.75-19.25	53.604	44.353	17.3
19.25-19.75	59.521	76.012	-27.7

Table 2. Here we show our dust-corrected B-band number counts per degree squared per half magnitude for our NGC and SGC fields. We have also shown the number discrepancy (as a percentage) of the SGC data relative to the NGC data.

R	N_{gal}^{NGC}	N_{gal}^{SGC}	N-S discrepancy
11.25-11.75	0.019	0.020	-0.5
11.75-12.25	0.094	0.043	54.3
12.25-12.75	0.113	0.079	30.1
12.75-13.25	0.211	0.152	28.0
13.25-13.75	0.379	0.331	12.7
13.75-14.25	0.676	0.509	24.7
14.25-14.75	1.309	1.036	20.9
14.75-15.25	2.810	1.956	30.4
15.25-15.75	5.315	4.136	22.2
15.75-16.25	10.294	7.683	25.4
16.25-16.75	19.157	15.078	21.3
16.75-17.25	33.120	28.317	14.5
17.25-17.75	54.423	49.305	9.4
17.75-18.25	84.271	82.154	2.5
18.25-18.75	113.543	124.624	-9.8

Table 3. Here we show our dust-corrected R-band number counts per degree squared per half magnitude for our NGC and SGC fields. We have also shown the number discrepancy (as a percentage) of the SGC data relative to the NGC data.

and 0.31 mag. to the APMBGC data. The DUKST corrected data is now significantly altered, but the counts are still much lower than the q_0=0.05 evolution model. We have also made a small dust correction to the APM and APMBGC data shown in Fig. 10. A standard A_B=C(cosec(b)-1) extinction law was originally assumed by Maddox et al. for the APM photometry, which corresponds to A_B=0 at the poles and a maximum A_B ∼0.03 mag. at $b = 50^{\circ}$, averaging ∼ 0.01 mag over the whole APM area. The Schlegel et al. (1998) dust maps, which are used to correct the 2dF counts and our own CTIO data, predict 0.02-0.03 mag. of extinction, even at the poles, and our average CTIO dust correction was 0.08 mag. in the SGC. We have therefore corrected the APM counts and the APMBGC data by an additional 0.08 mag (so the total correction is 0.08 mag. for the APM counts and 0.39 mag. for the APMBGC data). The original APM counts now show no galaxy number deficiency for B>18, but still indicates a large local hole at brighter magnitudes over a huge 4300 deg^2 area.

The 2dF data shown in Fig 10 shows excellent agreement with our CTIO data in both galactic caps. The 0.1 mag. zero-point correction we have applied to the 2dF NGC data now means that their north-south difference agrees with ours almost exactly for B<18. This agreement with our data in each galactic cap is interesting given the larger angular areas of 740 deg^2 and 1094 deg^2 of the 2dFGRS NGC and SGC fields respectively. Therefore it would seem that our survey areas of 242 deg^2 and 297 deg^2 are fairly typical samples of the galaxy distribution in these regions of the Universe.

5 NUMBER REDSHIFT DISTRIBUTIONS

5.1 The Durham/UKST N(z) Distribution

The zero-point discrepancy between the DUKST photographic plate photometry and that of our CCD based data has important consequences in terms of the DUKST number counts and n(z) distributions. We have used the "best sample" from Ratcliffe et al. (1998) using the uncorrected EDSGC photometry, taking into account the magnitude limits and completeness corrections of each of the 60 fields, in order to re-construct the DUKST n(z) distribution shown in Fig. 11. The average magnitude limit for the DUKST "best sample" over all 60 fields is b_J=16.86 and the dotted line shows the n(z) predicted using the Ratcliffe et al. (1998a) luminosity function parameters. This has been calculated using Ratcliffe's "best sample" magnitude limit, first brightened by 0.05 mag. to take account of the DUKST photometry relative to that of the EDSGC at b_J=19.5, and secondly 0.2 mag is added in order to convert to the B Landolt system. We therefore use $B_{lim} = 16.86 - 0.05 + 0.2 = 17.01$. In fact, this curve is equivalent to correcting all of the DUKST magnitudes by 0.24 mag. *and* the M* value in the luminosity function by the same amount as the two effects cancel each other out. The dashed line shows a prediction with the 0.24 mag. photometry correction applied to the magnitude limit, giving $B_{lim} = 17.01 - 0.24 = 16.77$, but with no alterations to the original value of the M* of Ratcliffe et al. (1998b).

Fig. 12 again shows the DUKST n(z) distribution but this time with predictions using the luminosity functions of

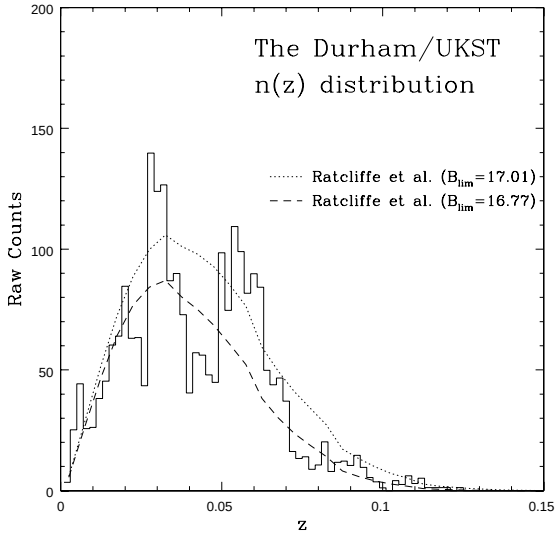

Figure 11. The plot shows the DUKST n(z) distribution, which has been constructed using the "best sample" from Ratcliffe et al. (1998) with the corresponding magnitude limits and completeness corrections for the raw EDSGC photometry in all 60 fields. The average magnitude limit of the 60 fields, taking into account the photometry correction applied by Ratcliffe et al. is b_J=16.86-0.05=16.81. The dotted line shows the prediction using the original luminosity function of Ratcliffe et al. (1998a) calculated from the data itself using the appropriate B Landolt magnitude limit of 16.86-0.05+0.20=17.01. The dashed line shows a prediction except with the 0.24 mag. photometry correction applied to the magnitude limit, giving $B_{lim} = 17.01 - 0.24 = 16.77$.

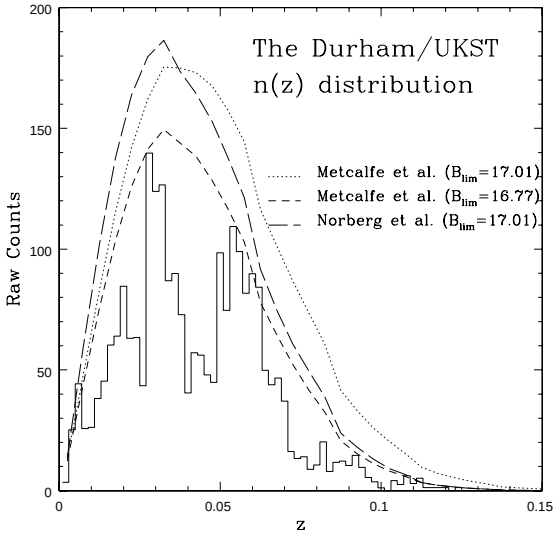

Figure 12. The DUKST n(z) distribution compared to predictions from other luminosity functions. The dotted line shows a prediction using the luminosity function of Metcalfe et al. (2001) calculated using the appropriate B Landolt magnitude limit of 16.86-0.05+0.20=17.01. The long dashed line shows a prediction from the new 2dFGRS luminosity function using the same magnitude limit (see text for more details of this luminosity function). Finally, the short dashed curve again shows a prediction using the luminosity function of Metcalfe et al. (2001) but calculated for the magnitude limit B_{lim}=16.77, which takes into account the 0.24 zero-point discrepancy found between our CTIO CCD data and the DUKST photographic photometry.

Metcalfe et al. (2001) and Norberg et al. (2001). The b_J luminosity function of Norberg et al. (long dashed curve) has been calculated using 110,500 galaxies from the 2dFGRS at z=0, taking account of evolution, the distribution of magnitude measurement errors and small corrections for incompleteness within the 2dF catalogue. We have used their published values of $M^\star_{b_J}$=-19.66 ($M^\star_B$=-19.46) and $\alpha = -1.21$. A $\phi^\star$=2.6x10^{-2}Mpc^{-3} was chosen so that the predicted galaxy number count from the Norberg et al. luminosity function matched that of the Metcalfe et al. model at B=19.5. We have also shown a prediction from the luminosity function of Metcalfe et al. (2001) using a magnitude limit of B_{lim}=17.01 (dotted curve) and the CTIO corrected magnitude limit of B_{lim}=16.77 (short dashed curve).

The predictions from the two luminosity functions agree reasonably well for z<0.05 but the Metcalfe et al. model predicts slightly more galaxies at higher redshift. However, both models clearly over-predict the DUKST n(z) at all redshifts. This clear deficiency of galaxies was originally considered surprising by Ratcliffe et al. given the DUKST covers 1500 deg^2 but it was thought that, because of the relatively bright magnitude limit of b_J=16.86 and shallow redshift depths, that significant large scale structure at low redshift could explain this. By taking into account the zero-point correction of 0.240 and using the Metcalfe et al. model with B_{lim} =17.01-0.240=16.77, we find that this apparent underdensity of galaxies is not as large as first thought. Even so the corrected Metcalfe et al. model still over-predicts the n(z) distribution at virtually all redshifts and so we draw a similar conclusion to that of Ratcliffe et al. in that, even after our photometry correction is applied, significant large scale structure is still observed in the DUKST n(z) distribution. The dashed line in Fig 12 shows this model which indicates that the deficiency of galaxies relative to the Metcalfe et al. model is still apparent until at least z=0.1 Relative to this photometry-corrected Metcalfe et al. model the DUKST n(z) distribution shows three clear holes in the galaxy distribution in the redshift ranges 0.005<z<0.025, 0.03<z<0.055 and 0.06<z<0.09 with number discrepancy percentages of ∼40 per cent, 45 per cent and 50 per cent respectively. In Section 6 we will analyse these apparent under-densities in more detail in conjunction with the results from the 2dFGRS n(z) distribution which we discuss in Section 5.

5.2 The 2dFGRS N(z) Distributions

The good photometry agreement in the SGC field between us and the 2dFGRS means that we are able to use the 2dF SGC n(z) distribution in conjunction with the galaxy count model of Metcalfe et al. (2001) described in 4.3, to perform a consistent analysis of the observed deficiency of galaxies in the SGC as a function of redshift. We can also make the appropriate zero-point correction in the NGC so we are then consistent with the 2dF photometry in order to investigate the 2dF NGC n(z) distribution.

We show the 2dFGRS n(z) distributions in Figs. 13

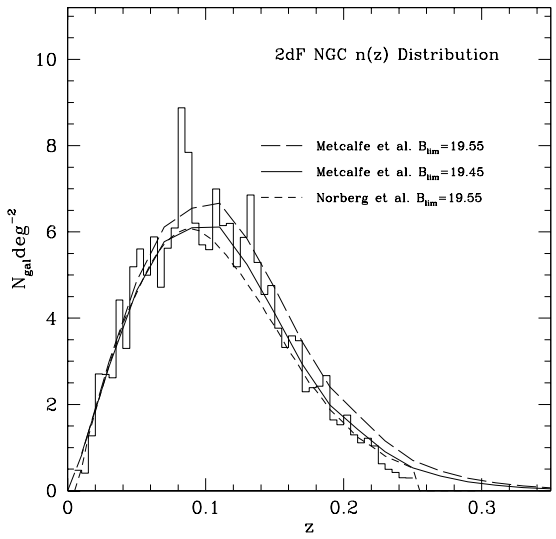

Figure 13. Here we show the n(z) distribution from the 2dFGRS in their NGC field along with two galaxy number count predictions using the luminosity function of Metcalfe et al. (2001) (solid and long dashed lines). We also show a prediction using the 2dF luminosity function (Norberg et al. 2001) (short dashed line). The mean magnitude limit of the APM-based photographic plates in the NGC is b_J=19.35 and so, assuming B-b_J=0.20 mag, we adopt a magnitude limit, m_{lim} of B=19.55 using each of the Norberg et al. and Metcalfe et al. models. The second prediction of the Metcalfe et al. model uses a magnitude limit corrected brighter by 0.1 mag. to B=19.45 in accordance with the zero-point difference we found between the 2dF NGC photometry and that of our CTIO data.

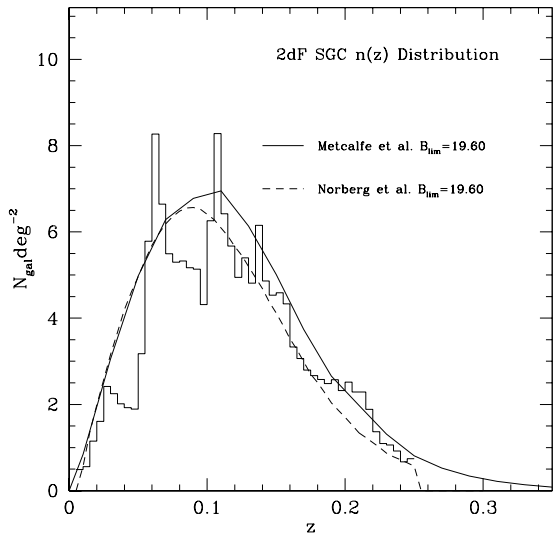

Figure 14. Here we show the n(z) distribution from the 2dFGRS in their SGC field and predictions using the luminosity functions of Metcalfe et al. (2001) (solid line) and Norberg et al. (2001) (dashed line). There are two clear "holes" in the 2dF SGC galaxy distribution in the ranges 0.03<z<0.06, with an under-density of ∼35-40 per cent, and 0.07<z<0.1 where the galaxy density deficiency is ∼25 per cent. The mean magnitude limit of the photographic plates in the SGC is b_J=19.40 and so, assuming B-b_J=0.20, we adopted a magnitude limit, m_{lim} of B=19.60 when computing the n(z) predictions.

and 14 obtained from the 100k data release (Colless et al. 2001). The mean magnitude limit of the 2dF photographic plates is b_J=19.35 and b_J=19.40 in the NGC and SGC respectively. Due to uncertainties in the effective areas and completeness, we have normalised the data such that the ratio of the predicted to the observed number of galaxies matches the corresponding ratio in the n(B) counts to the same magnitude limits. In Fig. 13 we have plotted three model curves, two of which use the Metcalfe et al. (2001) luminosity function (long dashed and solid curves) and a third which uses the luminosity function of Norberg et al. (2001) (short dashed curve) described in section 3.4.2. The long dashed and short dashed curves were both calculated using the appropriate mean magnitude limit, B_{lim}=19.55, of the APM-based plates in the NGC (assuming B-b_J=0.2). We only show the Norberg et al. model at B_{lim}=19.55, since any photometry correction would be also applied to the Norberg et al. M*; this would leave the n(z) virtually unchanged.

The models agree at low redshift but the B_{lim}=19.55 Metcalfe et al. model significantly over-predicts the data, particularly at the higher redshifts plotted. The solid curve, however, takes into account our zero-point correction derived in the previous section, equal to 0.1 mag. for b_J >16, and we therefore use a magnitude limit, B_{lim}=19.55-0.1=19.45. This model now shows excellent agreement with the observed NGC data and it is interesting that this zero-point correction is vital in order that the Metcalfe et al. model does not over-predict the data. This excellent agreement of the data with the Metcalfe et al. and Norberg et al. models at all redshifts, indicates that the galaxy distribution appears to be fairly uniform in the 2dF NGC field with no evidence for any huge under-densities as we saw for the DUKST field.

Fig. 14 shows the 2dF SGC n(z) distribution along with two model predictions using the Metcalfe et al. luminosity function (solid curve) and that of Norberg et al. (dashed curve). Our photometry comparison with the 2dF SGC data in the previous section showed up no significant zero-point error and so we used the appropriate magnitude limit of B_{lim}=19.60 for each model. The main result of these model comparisons so far has been that the Metcalfe et al. model predicts more galaxies at higher redshift and this case is no different, but the Metcalfe et al. model shows a slightly better agreement with the data than the Norberg et al. model which under-predicts the data for z>0.14. The most striking feature of the plot however is the two clear "holes" in the galaxy distribution in the ranges 0.03<z<0.055, with an under-density of ∼35-40 per cent, and 0.06<z<0.1 where the density deficiency is ∼25 per cent. We now analyse these underdensities in the galaxy distribution in more detail.

6 DISCUSSION

We have attempted to analyse the depth and angular size of the apparent "hole" in the SGC galaxy distribution using data from the APM, 2dFGRS, DUKST and 2MASS surveys. One of the major discoveries of this paper has been

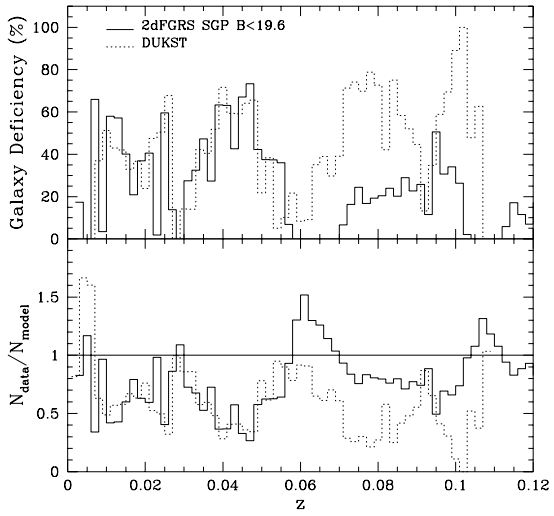

Figure 15. In the upper panel we show the galaxy number deficiency in the DUKST and 2dF SGC for B_{lim}=19.6 n(z) distributions plotted as a function of redshift. We have calculated this using the histograms in Figs. 12 and 14 relative to the appropriate prediction using the Metcalfe et al. (2001) luminosity function. We define the galaxy deficiency (in per cent), $D_g(z)$=100(N_{model}(z)-N_{data}(z))/$N_{model}(z)$ where N_{data} is the number of galaxies from the appropriate survey data and N_{model} is the number predicted from the model of Metcalfe et al. The lower panel illustrates the ratio of the quantity N_{data}/N_{model} for the DUKST and 2dF SGP fields, also as a function of redshift.

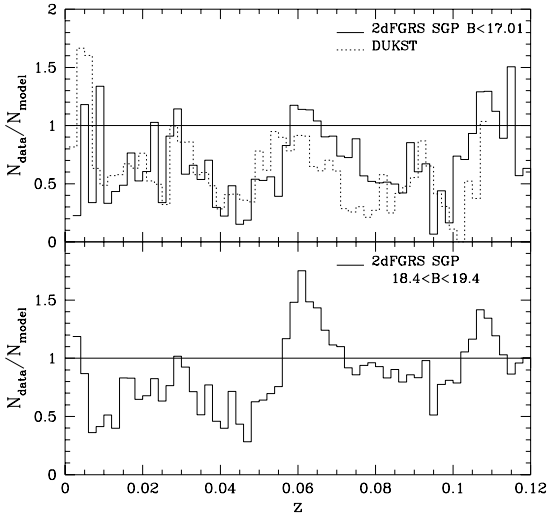

Figure 16. In the upper panel the histogram shows the the ratio of the quantity N_{data}/N_{model} for the 2dFSGC n(z) distribution with an imposed magnitude limit of B=17.01, relative to the appropriate prediction using the the Metcalfe et al. (2001) luminosity function. The dotted histogram shows the DUKST n(z) as in Fig. 15. The lower panel shows the same ratio for the 2dFGRS for 18.4<B<19.4 relative to the Metcalfe et al. model with the same limits.

the large galaxy-number deficiency relative to the Metcalfe et al. model in the DUKST and 2dF n(z) distributions. In fact there are distinct similarities between the two n(z) distributions which we attempt to quantify in Fig. 15. There are two panels in these histogram plots where the upper panel shows galaxy number deficiency vs redshift and the lower panel shows N_{gal}/N_{model} again vs redshift. We define the percentage galaxy number deficiency as:

$$D_g(z) = 100\frac{(N_{model}(z) - N_{data}(z))}{N_{model}(z)} \quad (9)$$

where N_{model} is the number of galaxies predicted using the Metcalfe et al. (2001) luminosity function and N_{data} is the number of galaxies from the appropriate survey data. In each panel, predictions for the DUKST survey are shown by the solid lines and those of the 2dFGRS by the dashed line. In the upper panel the four holes found in the DUKST n(z) distribution are clearly illustrated by the four peaks in the solid histogram with the two peaks of the dashed histogram showing the under-densities found in the 2dF SGC n(z).

The similarity between the 2dF and DUKST n(z) distributions is quite striking. The two under-densities seen in the 2dF SGC n(z) in the redshift ranges 0<z<0.055 and 0.06<z<0.1 are also clear features in the DUKST n(z). In fact, the galaxy discrepancy in the range 0<z<0.055 for the two surveys is almost the same magnitude in size with the histograms showing a very similar shape. The second under-density in the 2dF SGC n(z) is less pronounced than its DUKST counterpart, but they still cover very similar redshift ranges. The rise in the galaxy number density between the two 2dF SGC under-densities is also seen in the case of the DUKST survey. Given that the 2dF SGC field is entirely contained within the areas of sky observed for the DUKST survey we claim that the the similarities we have described in the two n(z) distributions are both artefacts of the *same* features in the galaxy distribution. Since the DUKST observes a larger 1500 deg^2 region than the 2dFGRS (who have redshifts for galaxies covering ∼300 deg^2 in the SGC at present) it could be that there is significant large scale structure observed by DUKST that is not seen by the 2dFGRS explaining the larger and more numerous galaxy number discrepancies in the DUKST n(z) distribution.

But there is evidence for an alternative explanation. For z>0.06 shown in the lower panel of Fig. 15, the DUKST survey shows significantly larger galaxy number discrepancies than the 2dFSGC n(z) relative to the Metcalfe et al. model. It is possible that galaxies can be biased tracers of the overall mass distribution and that intrinsically more luminous galaxies are then predicted to show stronger clustering properties, with regions of very high and low galaxy number densities. We suspect that the SGC might be under-dense and therefore the fact that the DUKST samples intrinsically brighter galaxies than the 2dF over all redshifts shown in Fig. 15, may mean that we are seeing the effects of bias.

Since this clearly needs further investigation, we have examined how the galaxy distribution varies with apparent magnitude. The results are shown in Fig. 16. In the upper panel we have plotted N_{data}/N_{model} for the 2dFGRS SGC data relative to the Metcalfe et al. (2001) model, each with an imposed magnitude limit of b_J=16.81 (B=17.01) to match the DUKST limiting magnitude. The DUKST n(z)

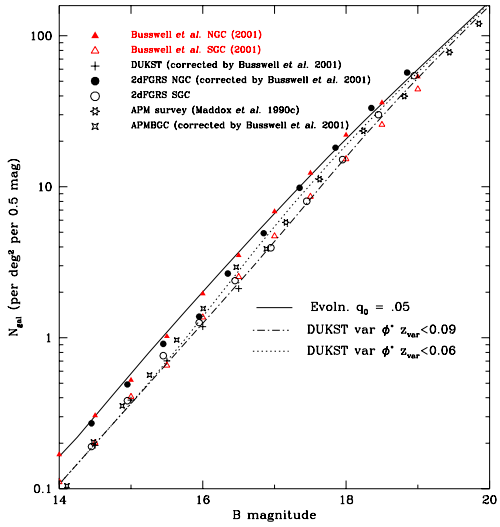

Figure 17. Here we show a similar plot to Fig 10 with the 0.313, 0.24 and 0.1 photometry corrections derived for the APMBGC, DUKST and 2dF NGC data respectively. We have also plotted four variable $\phi^\star$ models shown by the short dashed, dot-dashed, dotted and long-dashed curves, where the value of $\phi^\star$ is a function of redshift (see text for detailed expanation).

is indicated as in Fig. 15 by the dotted histogram for reference. It is very interesting that we now see a better agreement between the 2dF and DUKST n(z) for z>0.06. Similarly, in the lower panel we have imposed magnitude limits of 18.4<B<19.4 on the 2dFGRS SGC data and the Metcalfe et al. prediction in order to examine whether the galaxy number deficiencies seen in the bright data are compensated for by fainter galaxies. We can see from the lower panel of Fig. 16 that there is no significant effect for z<0.06, while the galaxy distribution for z>0.06 indicates a significantly reduced galaxy deficiency. This is entirely due to the different galaxy selection criterion we have used via the two magnitude limits of B<17.01 and 18.4<B<19.4, and suggests that the intrinsically brighter galaxies are clustered more strongly on $\gtrsim 50\,h^{-1}$ Mpc scales, despite the fact that the amplitude of the underdensities at z<0.06 remain the same; the galaxies here are sub-L* in both samples with approximately similar space densities, and so even this result may be in accordance with the notion of bias.

Fig. 17 shows our B-band galaxy number counts and our corrected APMBGC, 2dF and DUKST counts (see Fig. 10). For clarity, the bright original APM (B<17) counts have been removed since we have no reliable photometry checks using our CTIO data here, and the faint-end Metcalfe et al. corrected APM counts are shown with our corrected APMBGC counts. These counts are shown with respect to two variable $\phi^\star$ models where the value of $\phi^\star$ is a function of redshift instead of the usual constant value defined from the Metcalfe et al. (2001) B-band luminosity function. In these models the $\phi^\star$ is determined for certain low redshift ranges ($z \leq z_{var}$) by multiplying the usual Metcalfe et al. (2001) value by the factor $N_{data}(z)/N_{model}(z)$ for the bin widths shown in Fig. 15. For $z > z_{var}$ the usual Metcalfe et al. (2001) $\phi^\star$ is used.

The motivation for these variable $\phi^\star$ models is to locate the structure in the n(z) which dominates the bright galaxy counts. Recall that the DUKST n(z) indicates three distinct deficiencies in the galaxy distribution below z≈0.1. The DUKST z_{var} <0.09 and z_{var} <0.06 models were constructed then in order to see the effect on the predicted number counts, assuming that just the first two and then all three of these holes have significant effects on the galaxy counts.

The z_{var} <0.09 model fits the bright Southern CTIO counts well but slightly underpredicts the APMBGC data. The z_{var} <0.06 overpredicts the Southern CTIO counts. Since this redshift range appears to be unaffected by bias this indicates that the deficiency in the Southern CTIO counts is caused by structure to $z \lesssim 0.1$. The fact that the z_{var} <0.09 model slightly underpredicts the APMBGC counts indicates that the galaxy deficiency of the hole may be less over the whole SGC than the ≈30 per cent indicated in the counts from the DUKST, 2dFGRS SGC and Southern CTIO strips. A comparison of the APMBGC counts in Fig. 17 with the homogeneous model still indicates a 25 per cent deficiency over the full 4300 deg^2 of the APM Southern Survey. The conclusion from these variable $\phi^\star$ models then is that the Southern B-band counts are most consistent with there being a galaxy number discrepancy for $z \lesssim 0.1$, which is of order ≈25 per cent.

These results agree very well with those of Frith et al. (2003), who investigated the angular extent of the hypothesised deficiency of galaxies in the SGC using the publicly available 2MASS second incremental release data. The authors took 5° declination slices in the NGC and SGC with RA ranges similar to that of the 2dF regions, and plotted galaxy number counts in the K-band. In total twelve declination slices of data, each of $\sim 300-400$ deg^2, were analysed totalling ~ 4300 deg^2 from the two Galactic Caps. Since the APM, 2dF SGC and DUKST survey areas overlap with the three of the southern 2MASS strips, the work done by Frith et al. is extremely relevant to the discussion in this paper. Their conclusions also show strong evidence for a significant under-density of ≈30 per cent in the galaxy number density in their SGC areas. This agrees well with the 25 per cent deficiency that we have shown in this paper is implied by the APM and APMBGC data. The DUKST field then extends further south than is currently sampled by 2MASS, to δ=-43° and the APM area even further to δ=-70°. This then implies a hole in the SGC galaxy distribution of 100°x60°, which extends to z≈0.1. This corresponds to a huge volume of space of ≈10^7 h^{-3} Mpc^3 and implies significant power on large scales of ∼100-200 h^{-1} Mpc.

To illustrate how excess power on larger scales increases the chances of finding a 25 per cent galaxy deficiency over these volume sizes, we have used the 3-D analogue of equation 45.6 in Peebles (1980). By assuming a power law form of the spatial two-point correlation function out to a given scale length, we can calculate the probability of finding a given number deficiency of galaxies over a volume of space defined by a sphere of radius $150h^{-1}$Mpc. In this simplified scenario, the fluctuation in galaxy number over the expected galaxy number can be written as:

$$\frac{< (N-\bar{N})^2 >^{\frac{1}{2}}}{\bar{N}} = \frac{\left(1 + \frac{4\pi}{V}\int_0^{r_s} \xi(r) r^2 dr\right)^{\frac{1}{2}}}{\bar{N}^{\frac{1}{2}}} \qquad (10)$$

where $\xi(r)$ is the two-point spatial function and V is the volume of the sphere over which a particular survey is sampling. If we write $\frac{<(N-\bar{N})^2>^{\frac{1}{2}}}{N}=\frac{\delta N}{N}$ then:

$$\frac{\delta N}{\bar{N}} = \left(\frac{1}{\bar{N}} + \frac{3}{r_s^3}\left[\frac{r_0^{1.8} r_{cut}^{1.2}}{1.2}\right]\right)^{\frac{1}{2}} \quad (11)$$

where we assume the galaxy correlation length in proper coordinates, r_0=5.0h^{-1}Mpc, r_{cut} in Mpc is the length scale to which we assume the power law form of the correlation function extends, r_s=150h^{-1}Mpc and is the radius of the sphere defining our volume, $\bar{N}$ is the expected number of galaxies in this volume and $\delta N/\bar{N}$ is the expected fluctuation in the galaxy number. We assume two cases, each corresponding to a different value of r_{cut}. In the first case r_{cut}=10h^{-1}Mpc. If we set $\bar{N}=(4\pi r_s^3\bar{n})/3$, where we assume $\bar{n}$=0.01 which is the mean galaxy density in units of h^3Mpc^{-3}, then we find that $\delta N/\bar{N}$=0.016. This corresponds to an expected galaxy number fluctuation over our sphere of radius 150h^{-1}Mpc of 1.6 per cent and therefore means that finding a galaxy number deficiency of 25 per cent over our sphere is a 15.6σ result, although it is difficult to judge how much the *a posteriori* selection is affecting this result.

However, if we assume our second case where r_{cut}=150h^{-1}Mpc then we find an expected galaxy number fluctation of 8 per cent. This is a 3.75σ result and so a power law correlation function extending to 150 h^{-1} Mpc is starting to be more consistent with the observation of the local underdensity.

We take the ΛCDM real-space correlation function of Padilla & Baugh (2003), which we have modelled by two power laws of γ=-1.7 and γ=-3.44 with a break at r_{break}=30 h^{-1} Mpc. This overestimates the ΛCDM $\xi(r)$ at all scales for r$\gtrsim$ 100 h^{-1} Mpc. Even so, integrating this model to r_s=150 h^{-1} Mpc, we find that a 1σ fluctuation is of order 4.8 per cent indicating that our 25 per cent observed fluctuation is a 5σ deviation.

We conclude that there may be more power required at large scales than in the ΛCDM $\xi(r)$; although biasing the galaxy distribution could improve the agreement, in standard versions of the ΛCDM model the galaxy distribution is predicted to be unbiased on large scales. The implied excess power is also in contradiction with the currently observed forms for the APM and 2dFGRS correlation functions (Hawkins et al. 2002). Either these correlation functions have underestimated the amount of power at large scales or the galaxy distribution in the SGC is atypical of the overall distribution of galaxies. We are therefore currently reanalysing the correlation functions of the 2dFGRS to check whether any such problem exists (Frith et al., in preparation).

7 CONCLUSIONS

In this paper we first presented the resulting galaxy counts from our CTIO Curtis Schmidt data. The large deficiency of galaxies seen in the SGC motivated us to investigate the possible existence of a large "hole" in the SGC galaxy distribution. Using our CTIO data, covering 300 deg^2 in the SGC, we were able to make the first ever detailed checks of the bright (B<17) galaxy photometry in the DUKST, 2dFGRS and APM surveys which has crucial implications for the existence of a local hole in the distribution of galaxies. Our conclusions are:

- Our B-band galaxy counts in the NGC agree extremely well with the model of Metcalfe et al. (2001) but our SGC counts shows a significant galaxy deficiency, a mean 30.7 per cent in the magnitude range 14<B<18.5.
- Good agreement is found for our NGC data with the SDSS and MGC number counts in the magnitude interval 16.5<B<18.5 and likewise for our SGC galaxy counts with the data of Bertin & Dennefeld and the APM survey in the range 16.5<B<19.
- We compared our CCD galaxy catalogue to that of the 2dFGRS in the NGC and SGC. In the NGC we find good agreement of the zero-point at b_J=16 but our galaxies are, on average, 0.13 mag. brighter at b_J=18 implying a scale error of 0.065 mag/mag. We find a mean zero-point difference of 0.1 mag. in the range 16<b_J<18. In the SGC we find no zero-point or scale errors.
- After applying this 0.1 mag. zero-point correction to the 2dF NGC photometry we then find excellent agreement in both galactic caps between our CTIO data and the 2dFGRS, who's zero-point corrected results also imply a 30 per cent normalisation difference between the NGC and SGC galaxy counts at B=18.
- After comparing our CTIO photometry to both the DUKST and APMBGC data we found that our galaxies were, on average, brighter by 0.24 mag. and 0.31 mag. respectively.
- Our R-band galaxy counts show a normalisation difference for the NGC and SGC data of ∼22.2 per cent in the range 13<R<17.
- The 2dF and DUKST n(z) distributions show striking common structure with regard to 2 "holes" in the galaxy distribution in the redshift ranges 0.03<z<0.05 and 0.06<z<0.09, with number discrepancy percentages of 35-50 per cent , 25-60 per cent respectively.
- The DUKST survey finds significantly larger galaxy number discrepancies for z>0.06 than the 2dF survey in the SGC. This is evidence that bright galaxies may be biased tracers of the underlying mass distribution.
- Using variable $\phi^\star$ models based on the structure seen in the DUKST and 2dFGRS n(z)'s we claim that the galaxy count data is consistent with there being a hole in the SGC galaxy distribution over the whole 4300 deg^2 APM area, which extends out to z=0.1.
- Taking together the deficiency in the APMBGC counts and our variable $\phi^\star$ models we conclude that there is a galaxy number deficiency of ≈25 per cent over a huge angular area of 100°x60° in the SGC. The evidence is that this hole extends out to z=0.1 or 300h^{-1}Mpc. This result agrees well with those of Frith et al. (2003)
- We show, using a simple model, that significant power is required in the two-point correlation function on very large scales if there is to be any reasonable chance of the existence of such a large hole in the galaxy distribution. The ΛCDM model shows less excess power than required to explain the existence of such a feature in the galaxy distribution unless it is significantly biased

on $\approx 150\,h^{-1}$ Mpc scales. This is not expected in current ΛCDM scenarios which are supposed to have b=1 for $r \gtrsim 1\,h^{-1}$ Mpc.

REFERENCES

Bertin, E. & Arnouts, S., 1996, A&AS, 117, 393
Bertin, E. & Dennefeld, M., 1997, A&A, 317, 43
Blanton, M.R. et al., 2001, AJ, 121, 2358
Busswell, G.S., 2001, Durham University Ph.D. Thesis
Colless, S. et al. 2001, MNRAS, 328, 1039
Collins, C.A., Heydon-Dumbledon, N.H. & MacGillivray H.T., 1988, MNRAS, 236, 7
Dalton, G.B., Efstathiou, G., Maddox, S.J. & Sutherland, W.J., 1995, MNRAS, 269, 151
Frith, W.J., Busswell, G.S., Fong, R., Metcalfe, N. & Shanks, T., 2003, MNRAS, submitted
Hawkins, E. et al. 2001, astro-ph/0212375
Landolt, A.U., 1992, AJ, 104, 372
Loveday, J., Peterson, B.A., Maddox, S.J. & Efstathiou, G., 1996, ApJS, 107, 201
Maddox, S.J., Sutherland, W.J., Efstathiou, G. & Loveday, J., 1990a, MNRAS, 243, 692
Maddox, S.J., Efstathiou, G. & Sutherland, W.J., 1990b, MNRAS, 246, 433
Maddox, S.J., Sutherland, W.J., Efstathiou, G., Loveday, J. & Peterson, B.A., 1990c, MNRAS, 247, 1
Metcalfe, N., Ratcliffe, A., Shanks, T. & Fong, R., 1998, MNRAS, 294, 147
Metcalfe, N., Shanks, T., Campos, A., McCracken, H.J. & Fong, R., 2001, MNRAS, 323, 795
Norberg, P. et al. 2001, astro-ph/0111011
Padilla, N.D. and Baugh, C.M. 2003, MNRAS, submitted
Peebles, P.J.E., 1993, Principles of Physical Cosmology, Princeton University Press
Picard, A., 1991, AJ, 102, 445
Pimbblet, K.A., Smail, I., Edge, A.C., Couch, W.J., O'Hely, E. & Zabludoff, A.I. 2001, MNRAS, 327, 588
Ratcliffe, A., Shanks, T., Parker, Q.A. & Fong, R., 1998a, MNRAS, 293, 197
Ratcliffe, A., Shanks, T., Parker, Q.A. & Fong, R., 1998b, MNRAS, 296, 173
Schlegel, D.J., Finkbeiner, D.P. & Davis, M., 1998, ApJ, 500, 525
Shanks, T. 1990, in The Galactic and Extragalactic Background Radiations, S. Bowyer & C. Leinert, Dordrecht:Kluwer, 269
Shectman, S.A. et al., 1996, ApJ, 470, 172
Stevenson, P.R.F., Shanks, T., Fong, R. & MacGillivray, H.T., 1986, MNRAS, 213, 953
Yasuda, N. et al., 2001, AJ, 122, 1104